Mutational Analysis of the Role of Hydrophobic Residues in the 338−348 Helix on Actin in Actomyosin Interactions†

Carl J. Miller,‡ Tim C. Doyle,§ Elena Bobkova,‡ David Botstein,§ and Emil Reisler*,‡

Department of Chemistry and Biochemistry and Molecular Biology Institute, University of California, Los Angeles, California 90095, and Department of Genetics, Stanford University School of Medicine, Stanford, California 94305-5120

Received November 7, 1995; Revised Manuscript Received January 19, 1996⊗

ABSTRACT: Yeast actin mutants with alanines replacing I341 and I345 were studied to assess the role of hydrophobic residues in the α-helix 338−348 in interactions with myosin. In structural models of the actomyosin complex, this helix on actin was assigned a prominent role in the strong binding of myosin to actin. Substitution of I341 with alanine reduced the strong binding of actin to myosin subfragment-1 (S1) 9-fold compared to wild-type actin. In addition, the V_{max} of the actin-activated S1 ATPase was reduced 4-fold with no change in the K_m. In contrast, substitution of I345 with alanine had no significant effect on either the strong binding to S1 or the actin activation of S1 ATPase. The I341A actin filaments were found to slide in the *in vitro* motility assays at a lower mean velocity (1.6 ± 0.4 μm/s) than wild-type actin filaments (2.6 ± 0.3 μm/s). Only 65% of the mutant actin filaments moved in such assays in comparison to 95% of the wild-type filaments. However, addition of 2.0 mM MgADP to the motility assay buffer induced movement of all the I341A filaments at a velocity (1.6 ± 0.1 μm/s) similar to that of wild-type actin (1.7 ± 0.1 μm/s). The decrease in motility of the I341A actin filaments in the absence of ADP was attributed to a negative load slowing the mutant filaments and the smaller force produced by the heavy meromyosin and I341A actin system. The latter conclusion was confirmed by showing that a greater percentage of NEM-modified heavy meromyosin (external load) was required for arresting the motion of wild-type actin in the *in vitro* motility assay than that needed for stopping the I341A filaments.

The interaction of myosin with actin in muscle contraction is thought to alternate between a weak and flexible interaction and a strong, force-generating binding. The weakly bound complexes are formed between actin and myosin with the bound MgATP or MgADP•P_i, while the strongly bound states include actomyosin in the absence of nucleotides (rigor) and with the bound MgADP. Elucidation of the actomyosin interface in both weak and strong states will clarify the transition between them. This, in turn, will facilitate the linking of specific structural properties to the kinetic and mechanical cycle of actomyosin.

Several recent biochemical and genetic studies have demonstrated that charged surface residues (1−4, 99−100, 24−25) on subdomain-1 of actin play an important part in the actomyosin interface during the weak binding of these proteins. Disruption of these sites affected the weak binding of myosin to actin, actin-activated myosin ATPase, and actin sliding in the *in vitro* motility assay (in the absence of methylcellulose) but had only a slight effect on the strong acto−S1 binding (Sutoh *et al.,* 1991; DasGupta & Reisler, 1992; Aspenstrom *et al.,* 1992; Adams & Reisler, 1993; Miller & Reisler, 1995). Similar analysis of actin residues participating in the strong binding of myosin subfragment-1 (S1)[1] is yet to be carried out.

Recent determination of actin and S1 structures (Kabsch *et al.,* 1990; Rayment *et al.,* 1993a) and subsequent modeling of the actomyosin interface identified the α-helix 338−348 on actin as the most likely site for the strong, stereospecific binding of myosin (Rayment *et al.,* 1993b; Schroeder *et al.,* 1993). This helix has a number of partially exposed hydrophobic residues including Ile341, Ile345, and Leu346 as well as a buried Trp340. A synthetic hydrophobic peptide of the region 338−348 was shown to bind S1 in the presence and absence of ATP (Labbe *et al.,* 1994), but evidence on the role of specific residues in the 338−348 helix in actomyosin function is still lacking. Initial characterization of the complementary site on myosin is resulting from the myosin cardiomyopathy mutation of Arg405. This residue is modeled to be an integral part of the region on myosin that interacts with the hydrophobic helix 338−348 on actin (Rayment *et al.,* 1993b; Schroeder *et al.,* 1993). Mutation of Arg405 reduced both the sliding velocity of actin filaments in the *in vitro* motility assays and the actin-activated ATPase activity of myosin (Cuda *et al.,* 1993).

In this study, we constructed several mutations in the 338−348 helix and characterized actin mutants with the Ile341 and Ile345 changed to alanine. Actin filaments with I341A substitution had decreased rigor myosin binding, reduced actin-activated ATPase, and slower sliding in the *in vitro* motility assays than wild-type actin. The decrease in the *in vitro* motility was linked to the smaller force generated by the I341A actin filaments with heavy meromyosin. The

† This work was supported by grants from the National Institutes of Health to E.R. (AR22031) and D.B. (GM46406 and GM46888), from the National Science Foundation to E.R. (MCB9206739), and by a USPHS National Research Service Award (GM 07185) to C.J.M.

‡ University of California, Los Angeles.

§ Stanford University School of Medicine.

⊗ Abstract published in *Advance ACS Abstracts,* March 1, 1996.

[1] Abbreviations: DNaseI, deoxyribonuclease I; F-actin, filamentous (polymerized) actin; G-actin, monomeric actin; HMM, heavy meromyosin; S1, myosin subfragment-1, NEM, *N*-ethylmaleimide.

0006-2960/96/0435-3670$12.00/0

decrease in force was attributed to a reduced transition from the weakly to strongly bound actomyosin state. In contrast, actin with Ile345 changed to Ala was not significantly affected in any of the myosin interaction properties.

MATERIALS AND METHODS

Reagents. Distilled and Millipore-filtered water and analytical grade reagents were used in all experiments. Dextrose, ATP, PMSF, DTT, phalloidin, *N*-ethylmaleimide, Rhodamine phalloidin, and β-mercaptoethanol were purchased from Sigma Chemical Co. (St. Louis, MO). Yeast extract and bactopeptone were purchased from Difco (Detroit, MI). DNaseI was purchased from Boehringer Mannheim (Indianapolis, IN). Restriction endonucleases and other DNA-modifying enzymes were purchased from New England Biolabs (Beverly, MA).

Plasmid Construction. All DNA manipulations were performed by standard techniques (Sambrook *et al*., 1989). A 5.5-kb *ACT1::HIS3*-containing *Eco*RI fragment from pKFW46 (Wertman *et al*., 1992) was ligated into the *Eco*RI site of pTD314 [an unpublished derivative of pRS314 (Sikorski & Hieter, 1989), in which the *Bsa*I and *Bcg*I sites have been removed from the bacterial *bla* gene] to give pTD24. This construct contains the *ACT1* orientated with respect to the f1 *ori* such that single-strand generation with helper phage yields the antisense strand of *ACT1*. In addition, this plasmid and its derivatives contain the yeast centromeric sequences *CEN6/ARS4* to allow retention in yeast cells, with appropriate selection, at low copy number.

Site-Directed Mutagenesis of the Actin Gene. Mutagenesis was performed by a modification of the method of Kunkel (Kunkel *et al*., 1987). pTD24 was transformed into the *E. coli* strain CJ236 [*dut1 ung12 thi-1 relA1* (pCJ105[*cam*^{r}F'])(Kunkel *et al*., 1987)] to allow the generation of uracil-containing DNA. Single-stranded plasmid DNA (ssDNA) was made by growing the cells to $OD_{600} = 0.1$ in 12 mL of LB medium and adding M13K07 helper phage to 1×10^{10} pfu and uridine to 1 μg/mL. After incubation at 37 °C for 75 min, 38 mL of 2 × TY medium, containing 50 μg/mL ampicillin, and 50 μl of 50 mg/mL kanamycin were added and incubated overnight at 37 °C. The bacteria were sedimented by low-speed centrifugation, and 10 mL of 2.5 M sodium chloride/20% (w/v) PEG8000 was added to 45 mL of the supernatant. Phage containing ssDNA were precipitated by centrifugation at 8000 rpm, and the pellet was resuspended in 500 μL of TE (10 mM Tris-HCl, pH 8.0, 1 mM EDTA). Following a further centrifugation at 13 000 rpm to remove any bacteria, the ssDNA was extracted by twice mixing with Tris-HCl (pH 8.0)-buffered phenol, twice with phenol/chloroform, and once with chloroform. The ssDNA was finally ethanol-precipitated, dried, and resuspended to 1 μg/μL in TE.

Oligonucleotide-directed mutagenesis was performed using oligonucleotides which either were purchased from Genset Corp. (San Diego, CA) or were a gift from Operon Technologies, Inc. (Alameda, CA). The oligonucleotides were 5′ phosphorylated using polynucleotide kinase (Sambrook *et al*., 1989); 0.5 pM ssDNA template pTD24 was mixed with 6.2 pM oligonucleotide in 25 μL of annealing buffer (40 mM Tris-HCl, pH 7.5, 20 mM $MgCl_2$, and 50 mM NaCl), heated to 80 °C for 2 min, and allowed to cool slowly to room temperature. Twenty-five microliters of polymerization mixture (10 mM dithiothreitol, 2 mM dNTP mix, 2 mM ATP, 0.5 mg/mL BSA, 200 units of T4 ligase, and 5 units of T7 DNA polymerase) was then added, and the mixture was incubated for 60 min at 37 °C. The reaction was stopped by the addition of 2 μL of 0.5 M EDTA, and 5 μL of the reaction mixture was used to transform the *E. coli* strain DH5αF'. Dideoxy-chain termination DNA sequencing (Sanger *et al*., 1977) was used to confirm replacements in all mutated plasmids.

Yeast Strain Construction. The strain used in this study for the expression of the mutant actin alleles was KWY201 [Wertman *et al*. (1992); referred to as DBY5532 in our collection], a diploid strain of genotype *ura3−52*/*ura3−52*, *leu2−3*,112/*leu2−3,112*, *his3*Δ*200*/*his3*Δ*200 ade2−101*/*ADE2*, *ade4*/*ADE4*, *can1*/*CAN1*, *TUB2*::*ACT1*/*tub2-201-(ben*^{r}*)::act1*Δ1::LEU2. The cultivation and manipulation of this strain and transformants followed standard methods (Kaiser *et al*., 1994). Yeast were transformed with plasmid DNA with the lithium acetate method (Ito *et al*., 1983), and transformants were selected and maintained by histidine selection. Transformants were sporulated and dissected to yield segregants from which mutant actin alleles were selected based on leucine and histidine independence. Since these segregants are not viable without the plasmid (the plasmid-borne actin being essential), strains were maintained without selection on nutrient-rich YEPD medium following selection. Haploid segregants were grown to exponential phase, and equal volumes were spotted onto YEPD or YEPD containing 900 mM sodium chloride, and grown at 14, 17, 25, 30, 35.5, and 37 °C to determine temperature and salt sensitivity of the actin mutants.

Preparation of Proteins. Actin was isolated from each strain using DNaseI affinity chromatography as previously described (Cook *et al*., 1993). Rabbit actin and myosin were prepared from rabbit skeletal muscle according to the methods of Spudich and Watt (1971) and Godfrey and Harrington (1970), respectively. Myosin subfragment-1 was prepared according to Weeds and Pope (1977).

Circular Dichroism and Tryptophan Fluorescence. Secondary structures of the I341A and wild-type G-actins (3.0 μM) were compared in circular dichroism (CD) experiments. The ellipticities of actin were measured in a Jasco J-600 CD spectropolarimeter between 190 and 250 nm in G-actin buffer (5 mM Tris, pH 7.6, 0.2 mM $CaCl_2$, 0.2 mM ATP, and 0.5 mM β-mercaptoethanol) at 25 °C. The emission spectra for tryptophan fluorescence were recorded with the Spex Flourolog (Spex Industries Inc., Edison, NJ) between 310 and 450 nm, by setting the excitation wavelength to 295 nm. The spectra were obtained at 23 °C in G-actin buffer.

Polymerization of Actins. Polymerization of each of the actins (5.0 μM) by 3.0 mM $MgCl_2$ in G-actin buffer was observed by measuring the light scattering at 325 nm in a Spex Flourolog spectrophotometer. The final light scattering values for the polymerized actin were measured following overnight incubation of samples.

Actin-Activated S1 ATPase Assays. Actin-activated ATPase activity was measured by using the malachite green assay (Kodama *et al.*, 1986). Because of the assay sensitivity, it was necessary to minimize free phosphate in the stock actin solutions (Sutoh *et al.*, 1991). Actins were polymerized in a solvent containing 4 mM $MgCl_2$, 5 mM KCl, 10 μM phalloidin, and 10 μM imidazole at pH 7.4 and centrifuged in a Beckman airfuge for 15 min. The resulting pellet was

dispersed in the same buffer and used as F-actin. Actin samples at final concentrations from 2 to 30 μM were preincubated with 0.4 μM S1 for 20 min in ATPase buffer (5 mM KCl, 2 mM $MgCl_2$, and 10 mM imidazole, pH 7.4). The ATPase reaction was initiated by addition of ATP to 1 mM final concentration. The reactions were stopped with an equal volume of 0.6 M perchloric acid and then diluted appropriately while maintaining a final concentration of 0.3 M perchloric acid. The mixture was centrifuged at 14 000 rpm for 10 min in a microcentrifuge to remove precipitated proteins. The amount of released phosphate was determined, and the activity of S1 alone was subtracted from each value.

In Vitro Actin Motility Assays. The motility assays were performed as previously described (Miller *et al.*, 1995) with a few modifications. Temperature was maintained at 25 °C for all assays. HMM was prepared as described by Kron *et al.* (1991). In order to remove ATP-insensitive heads, HMM was centrifuged with 0.15 mg/mL phalloidin-stabilized actin in a solution containing 0.1 M KCl, 4 mM $MgCl_2$, and 3 mM MgATP for 20 min in a Beckman airfuge. Unless otherwise noted, the supernatant was applied to nitrocellulose-treated coverslips at an HMM concentration of 0.1 mg/mL. Rhodamine phalloidin-labeled actin filaments were added to the coated coverslips at 10 nM, and after 1 min, the unbound filaments were washed away with the assay buffer (25 mM KCl, 1 mM EGTA, 4 mM $MgCl_2$, 10 mM dithiothreitol, and 10 mM imidazole, pH 7.4). Movement was initiated with the assay buffer containing 1 mM ATP and an oxygen-scavenging system. Quantification of the sliding velocities was done with an Expertvision system (Motion Analysis, Santa Rosa, CA). The velocities of individual filaments with standard deviations of less than one-third of the average velocity were used for statistical analysis (Homsher *et al*., 1991) and were considered to move smoothly in the assay system.

NEM-HMM was prepared as described previously (Warrick *et al.*, 1993). The *in vitro* motility assay was performed as above with the following modifications. HMM and NEM-HMM at appropriate weight ratios were adsorbed to the assay surface for 2 min and washed off with 6 volumes of assay buffer to prevent contamination with NEM-HMM. Nonmoving filaments were determined by tracking the centroid of each filament image with the Expertvision system and charting its movement for 20 s.

Cosedimentation Assays. Cosedimentation assays for binding of S1 to 3.0 μM phalloidin-stabilized actin were carried out at 23 °C in 3 mM ATP, 3 mM $MgCl_2$, 25 mM KCl, and 10 mM imidazole, pH 7.4, as previously described (DasGupta & Reisler, 1992). When used, ATP was added after the incubation of proteins for 10 min. The concentration of S1 ranged between 5.0 and 23.0 μM. The protein samples were centrifuged in a Beckman airfuge at 140000*g* for 10 min. Similar assays were done for the strong binding of S1 to actin (4.0 μM) in the presence of 100 mM KCl, 4.0 μM phalloidin, and 10 mM imidazole, pH 7.4. Resuspended pellets and supernatants of each sample were examined on SDS−PAGE (Laemmlli *et al*., 1970). The pellets contained actin and S1 bound to it; unbound S1 was found in the supernatant. Under these conditions, S1 was not pelleted when centrifuged in the absence of actin. Gels were stained with Coomassie Blue, and the bands were quantified by a Biomed Instruments softlaser densitometer (Fullerton, CA) interfaced to an IBM-compatible 486 computer for integration of peak areas. The densitometric traces of pelleted protein bands were analyzed to determine the molar ratios of S1 bound to actin. Molar stain ratios for S1 and actin were obtained from appropriate calibration gels. The binding curves shown in the plots, which trace the calculated molar ratios of S1 bound to actin as a function of S1 concentration, were obtained by solving the quadratic binding equation and using the experimental concentrations of S1 and actin. The dissociation constants, K_d, used in these calculations were obtained from Scatchard plots of the binding data.

Table 1: I341 and I345 Actin Mutants[a]

actin allele	mutation	nucleotide sequence (341−345)	phenotype
ACT1	none	ATT GGT GGT TCT ATC	(wild type)
act1−45	I341A	GCC GGC GGT TCT ATC	wild type
act1−53	I345A	ATT GGT *GGA TCC* GCC	wild type
act1−47	I341A/I345A	GCC GGC GGT TCT GCC	lethal[r]
act1−60	I341K/I345K	AAA GGT *GGA TCC* AAA	LETHAL[d]
act1−65	I341F	TTT GGT *GGA TCC* ATC	LETHAL[d]
act1−69	I345F	ATT GGT *GGA TCC* TTT	lethal[r]

[a] List of actin mutations generated in this study. Nucleotide alterations resulting in amino acid changes (underlined) and conserved mutations introducing a unique *Bam*HI site (italicized) are shown. Phenotypes of mutations in haploid cells are indicated with respect to the wild-type actin gene on the plasmid pTD24 (LETHAL[d], allele lethal in diploid cell, and dominant to the chromosomal *ACT1* allele; lethal[r], allele lethal only in haploid cell, and recessive to the *ACT1* allele).

RESULTS

Construction of Mutations. Construction of the novel mutations reported in this study utilized the same yeast strain and *HIS3*-marked *ACT1* DNA fragment as previously used (Wertman *et al*., 1992) to generate a synoptic set of site-directed mutations of the *ACT1* gene. However, rather than construct the mutations in the *E. coli* plasmid pUC119 (Vieira & Messing, 1991), the yeast centromeric plasmid [pTD314, a derivative of the pRS314 plasmid (Sikorski & Hieter, 1989), lacking the *Bsa*I and *Bcg*I sites within the *bla* gene], also containing the f1 *ori* to allow generation of single-stranded DNA, was selected to enable a simple transformation into yeast.

The 5.5-kb *Eco*RI fragment containing the *ACT1* gene marked downstream with the *HIS3* gene was excised from pKFW46 and ligated into the *Eco*RI site within the multiple cloning site of pTD314 to generate pTD24, and site-directed mutagenesis was performed on this new construct. Residues Ile341 and Ile345 were substituted as single or double mutants to alanine, phenylalanine, or lysine. Mutations were confirmed by sequencing, and transformed into the strain DDY5532 selecting for histidine independence. Plasmids which failed to generate transformants after repeated attempts were assumed to express a dominantly deleterious mutant actin protein (see Table 1; alleles *act1−60* and *act1−65*, I341K/I345K and I341F, respectively). Viable transformants were sporulated and dissected to generate haploid segregants, of which two of the spores of each tetrad would contain the wild-type chromosomal actin allele, and thus the viability of the other spore pair would be dependent on expression of a functional actin protein from the plasmid. Two of the transformants (Table 1, *act1−47* and *act1−69*, I341A/I345A and I341F, respectively) showed 2:0 tetrad viability, and further analysis confirmed that the viable segregants were leucine and histidine auxotrophs, and thus contained the

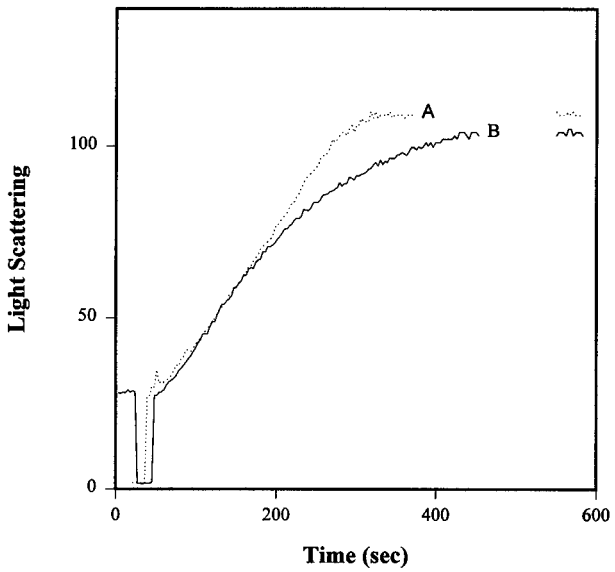

FIGURE 1: Polymerization of wild-type and mutant actins. The polymerization of 5.0 μM wild-type (A) and I341A mutant (B) G-actins by 3.0 mM $MgCl_2$ in G-actin buffer (5 mM Tris, pH 7.6, 0.2 mM $CaCl_2$, 0.2 mM ATP, and 0.5 mM β-mercaptoethanol) was monitored by the increase in light scattering from actin solutions. The polymerization was observed for 10 min for each actin.

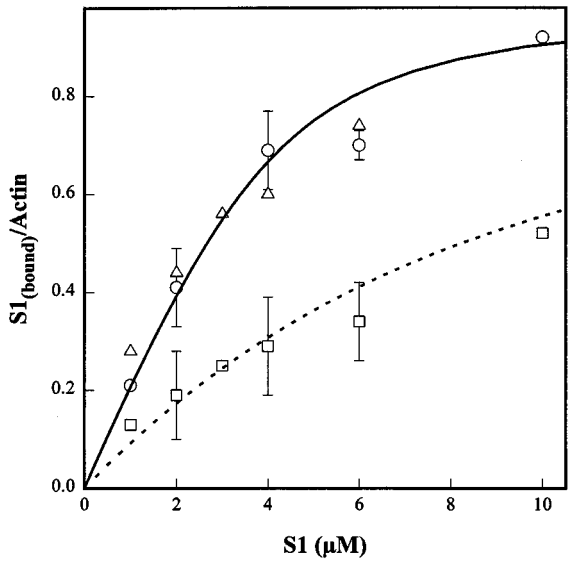

FIGURE 2: Binding of S1 to wild-type and mutant actins under rigor conditions. Mixtures of F-actin (4.0 μM) and S1 (between 1.0 and 6.0 μM) were preincubated in 100 mM KCl, 4.0 μM phalloidin, and 10 mM imidazole, pH 7.4 at 22 °C, and then pelleted in a Beckman airfuge. Supernatants and resuspended pellets were run on SDS−PAGE and quantified by densitometry. The molar ratios of S1 bound to wild-type actin (○) and I345A actin (△) are described by a single calculated binding curve (solid curve) corresponding to $K_a = (1.5 \pm 0.2) \times 10^6$ M^{-1}. The calculated dashed binding curve, $K_a = (1.6 \pm 0.5) \times 10^5$ M^{-1}, describes the binding of S1 to I341A F-actin (□). Error bars represent the standard deviation from three independent experiments.

chromosomal *ACT1* allele. The non-viable spores must contain recessive lethal mutations expressing a defective actin protein.

Only single alanine substitutions at both sites (Table 1, alleles *act1−45* and *act1−53*, I341A and I345A, respectively) were able to support growth of haploid yeast segregants when expressed as the sole actin. Strains expressing these mutant actins were neither heat nor cold sensitive, nor sensitive to the presence of high salt concentration, typical phenotypes of actin mutants (Ito *et al.*, 1983). Mutant actins were purified only from these two strains, which were free of wild-type actin.

Purification and Initial Characterization. Strains containing mutant and wild-type actin genes yielded similar amounts of actin protein after purification by DNaseI affinity column chromatography. These purified proteins were characterized in a number of ways (not all data shown). The tryptophan fluorescence of I341 and I345 mutant actins was compared to that of wild-type actin. A red shift of 3 nm, relative to wild-type actin, was detected in the emission spectrum (excitation wavelength = 295 nm) of the I341A mutant actin (to $\lambda_{max} = 334$ nm) but not in the I345A actin. Fluorescence intensities were the same for the three actins.

Significant changes in the secondary structure of the mutant actin were ruled out by CD experiments. The far-UV (between 190 and 250 nm) circular dichroism spectra of the I341A and wild-type actins were identical. This indicates that the small red shift in tryptophan fluorescence of the I341A actin is probably caused by the proximity of the altered residue to Trp340 and its local perturbation.

The ability of each actin to assemble into filaments was tested by measuring the increase in light scattering from actin solutions after addition of 3 mM $MgCl_2$. No significant difference in the rate or extent of polymerization was detected for either I341A (Figure 1) or I345A actins (data not shown) in comparison to wild-type actin. The wild-type and mutant actin filaments also appeared similar in their shape and length after labeling with rhodamine phalloidin and visualization with fluorescence microscopy.

Rigor and ATP-Sensitive Binding of Mutant Actins to S1. The affinity of mutant actins for myosin in both the absence and presence of ATP was tested in cosedimentation experiments. In the absence of nucleotides, the data for the binding of S1 to I341A mutant actin fitted to a calculated curve corresponding to a binding constant $K_a = (1.6 \pm 0.5) \times 10^5$ M^{-1} (Figure 2, dashed curve). The data for the binding of S1 to wild-type actin and I345A actin were not significantly different from each other and could be represented by a single curve corresponding to $K_a = (1.5 \pm 0.2) \times 10^6$ M^{-1} (solid curve). Thus, the mutation of I341 reduced 9-fold the rigor acto−S1 binding constant while the substitution of I345 had no effect on the binding. Notably, the rigor binding of S1 to wild-type yeast actin is weaker than to skeletal α-actin by at least 1 order of magnitude.

The weak binding of each actin to S1 was also measured by cosedimentation experiments. In the presence of 3 mM MgATP, no difference was observed between the binding of S1 to wild-type or I341A mutant actin as both could be described by a single binding constant of $(1.8 \pm 0.3) \times 10^4$ M^{-1} (Figure 3). This indicates that I341 has an important role in the strong acto−S1 binding but does not impact their weak binding in the presence of ATP.

Actin-Activated ATPase Activities. Replacement of I341 with alanine resulted in a significant reduction of the actin-activated ATPase of S1 (Figure 4). A 4-fold decrease in the V_{max} was measured for the I341A actin (0.6 ± 0.1 s^{-1}, lower curve) relative to that for wild-type or I345A actins. The kinetic data for I345A and wild-type actins could be fitted by a single hyperbola ($V_{max} = 2.4 \pm 0.3$ s^{-1}, upper curve). The K_m for the I341A mutant actin (10.5 ± 5.4 μM)

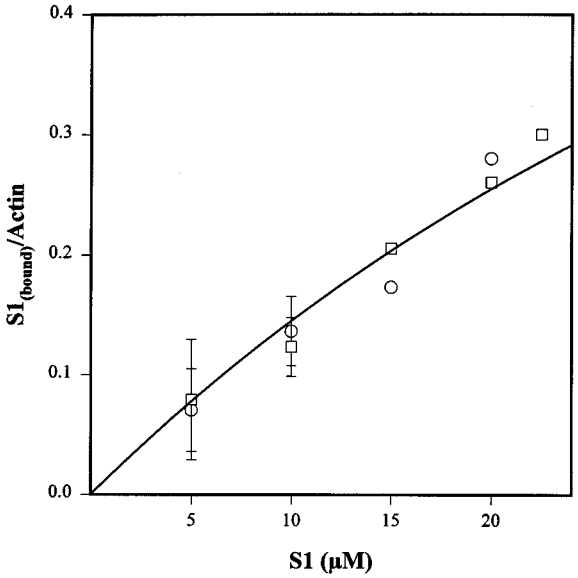

FIGURE 3: Binding of S1 to wild-type and mutant actins in the presence of MgATP. Mixtures of F-actin (3.0 μM) and S1 (between 5.0 and 22.5 μM) were pelleted in a solvent containing 10 mM imidazole, pH 7.4, 25 mM KCl, 1 mM EDTA, 3.0 mM MgATP, and 3.0 μM phalloidin at 22 °C in a Beckman airfuge at 140000*g* for 10 min. Supernatants and pelleted samples were run on SDS−PAGE and quantified by densitometry. The molar ratios of S1 bound to wild-type F-actin (○) and I341A F-actin (□) are described by a single calculated curve corresponding to $K_a = (1.8 \pm 0.3) \times 10^4$ M^{-1}. Error bars represent the standard deviation from three independent experiments.

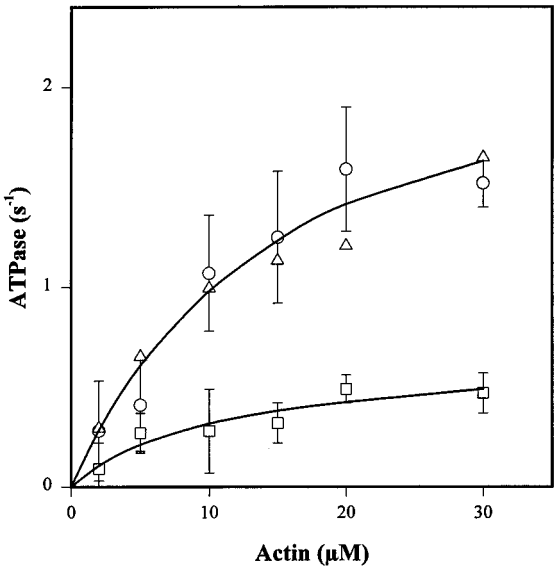

FIGURE 4: Actin-activated ATPase activities of S1 in the presence of wild-type and mutant actins. The activation of S1 ATPase by each actin was measured in the presence of between 2.0 and 30.0 μM phalloidin-stabilized F-actin, 0.4 μM S1, and 1 mM ATP in an assay buffer containing 10 mM imidazole, pH 7.4, 5 mM KCl, and 2 mM $MgCl_2$. Acto−S1 ATPase turnover rates were fitted to the Michaelis−Menten equation. The ATPase rates in the presence of wild-type actin (○) and I345A (△) are described by the upper hyperbola ($V_{max} = 2.4 \pm 0.3$ s^{-1}; $K_m = 15.0 \pm 6.8$ μM); the rates determined in the presence of I341A actin (□) are described by the lower hyperbola ($V_{max} = 0.6 \pm 0.1$ s^{-1}; $K_m = 10.5 \pm 5.4$ μM). Error bars represent the standard deviation from three independent experiments.

was not significantly changed compared to that for wild-type actin or I345A actin (15.0 ± 6.8 μM, Figure 4). This indicates that residue I341 is important for the catalytic

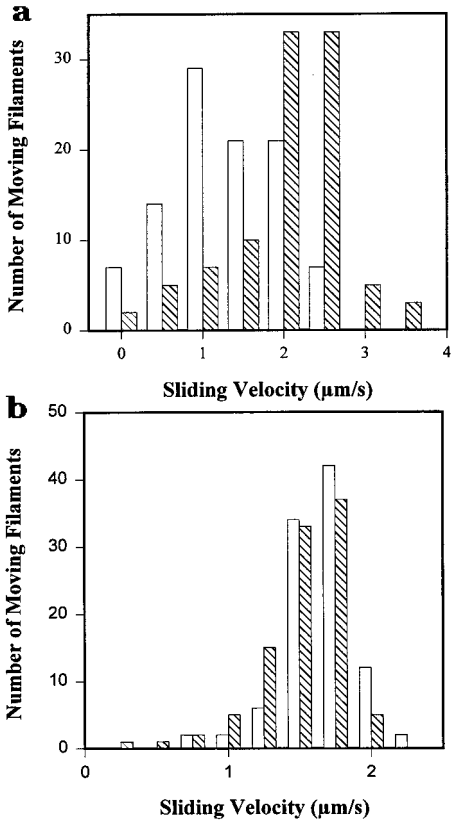

FIGURE 5: In vitro motilities of wild-type and I341A mutant actins. (a) *In vitro* motilities of I341A mutant actin (empty bars) and wild-type actin (striped bars) were measured over HMM adsorbed to a nitrocellulose-coated surface in the motility assay buffer (1 mM ATP, 10 mM imidazole, pH 7.4, 25 mM KCl, 1 mM EGTA, 4 mM $MgCl_2$, and 10 mM dithiothreitol). (b) *In vitro* motilities of I341A mutant actin (empty bars) and wild-type actin (striped bars) were measured in the motility assay buffer supplemented with 2 mM ADP.

interaction of actin and myosin, *i.e.*, the activation of myosin ATPase, but not for their binding in the presence of ATP.

Sliding Velocities of Filaments. The ability of the I341A and I345A actin filaments to slide over heavy meromyosin from skeletal myosin (HMM) was tested in the *in vitro* motility assays. Strikingly, at normal assay conditions (containing 1 mM MgATP), only 65% of the mutant I341A actin filaments translocated over the surface compared to nearly all of the wild-type actin filaments (>95%). The remaining 35% of the mutant actin filaments remained fixed at the HMM surface in a rigor-like manner irrespective of the presence of MgATP. The I341A actin filaments which did move in the assay had a mean sliding velocity of $V_s = 1.6 \pm 0.4$ μm/s compared to $V_s = 2.6 \pm 0.3$ μm/s for the wild-type actin filaments (Figure 5a). The I345A mutant actin moved similarly (95% moving, $V_s = 2.4 \pm 0.3$ μm/s) to wild-type actin. It is apparent that the I341A mutation impairs the movement of the actin filaments.

One possible explanation for the impaired motion of I341A actin filaments is that a mechanical load inhibits their sliding. It has been previously demonstrated that under the standard conditions of the *in vitro* motility assay [Materials and Methods; see also Kron *et al.* (1991)] an internal mechanical load can develop, probably as a result of photodamage to myosins (Haeberle, 1994, 1995). We tested for the presence of mechanical load in our system by inclusion of 2 mM ADP in the assay buffer. ADP was shown before to increase the

force generated in rabbit muscle fibers and decrease the velocities of fiber contraction (Pate & Cooke, 1989) and *in vitro* filament sliding. These observations were attributed to an increase in the population of A·M·ADP (actomyosin·ADP) crossbridges, and the inhibition of A·M (actomyosin) detatchment and the actomyosin ATPase cycle due to competition between ADP and ATP for the binding to A·M. Strikingly, ADP improved the motility of the I341A actin as the percentage of filaments sliding over HMM increased from 65% to 95%. The improvement in motility was also manifested in the smaller standard error of the mean sliding velocities in comparison to that in the absence of ADP (wild type, from 0.3 to 0.1 μm/s; I341A, from 0.4 to 0.1 μm/s). This indicates that ADP induced a more uniform motion of both types of actin filaments. The mean sliding velocity of I341A actins ($V_s = 1.7 \pm 0.1$ μm/s) was unchanged from that in the absence of ADP ($V_s = 1.6 \pm 0.4$ μm/s) while that of the wild type was reduced ($V_s = 1.6 \pm 0.1$ μm/s). This inhibition of wild-type actin sliding by ADP is consistent with the previous observation of competitive inhibition of the sliding of rabbit actin filaments in the *in vitro* motility assay (Homsher *et al.*, 1991; Warshaw *et al.*, 1991). Of particular interest is the ability of ADP to increase the percentage of I341A filaments moving in the assay and to improve their motion. This suggests that under normal assay conditions the I341A actin filaments were slowed and stopped because less force was generated. However, when the number of force-generating crossbridges was increased by ADP, the mutant actin sliding became indistinguishable from that of wild-type actin (Figure 5b).

Relative Forces of Actin Filaments in the in Vitro Motility Assay. To test for possible differences in the relative forces generated by I341A and wild-type actin filaments with HMM, a recently developed version of the *in vitro* motility assay was utilized (Haeberle, 1994; Warshaw *et al.*, 1992). This slight modification of the *in vitro* motility assay is based on the observation that inactivated, NEM-modified myosin, when mixed with unmodified myosin, inhibits filament motion. The load generated by NEM-HMM is due to its ATP-insensitive binding to actin. In this assay, the sliding is monitored at increasing ratios of load producing NEM-modified HMM to force generating unmodified HMM. As the ratio is increased, a progressive increase in the number of nonmoving filaments, an overall slowing of the filament motion, and an increase in filament fragmentation are all observed. These characteristics prevail until filament sliding is completely stopped. The ratio at which movement stops is distinguished by a transition from small (<1 μm), fragmented but still mobile filaments to long ($2-15$ μm), stationary filaments. The ratio of NEM-HMM/HMM at which this transition occurs in different actomyosin systems is determined by the ability of active crossbridges to generate force and overcome the load. Direct comparison of these ratios for the different actins enables the estimation of the relative force generated by different acto−HMM systems. Previously, this method has been used to illustrate the difference in forces generated by actin complexes with smooth and skeletal muscle myosins as well as to distinguish between the regulatory properties of thin filament associated proteins such as calponin, caldesmon, and tropomyosin (Haeberle *et al.*, 1994).

To examine the mechanical differences between I341A and wild-type actin filaments, we observed their sliding as the ratio of NEM-modified HMM/unmodified HMM was increased at small increments between 0 and 0.25. At all ratios, a smaller percentage of the I341A mutant actin filaments moved at slower velocities in comparison to wild-type actin (data not shown). Wild-type actin filaments were able to move up to, but not at, ratios of 0.21 NEM-HMM/HMM. In contrast, the motion of I341A mutant actin filaments was stopped at a ratio of 0.13 NEM-HMM/HMM. This difference corresponds to approximately a 40% decrease in the relative force generated along the mutant actin filament by HMM compared to the force obtained with wild-type actin filaments (or a ratio of $0.62 = 0.13/0.21$). This result is consistent with the explanation of the different motilities of I341A and wild-type actin filaments in terms of different forces generated in the two actin systems.

DISCUSSION

Structural models of acto−S1 (Rayment *et al.*, 1993b; Schroeder *et al.*, 1993) implicate the α-helix (338−348) on subdomain-1 of actin as a main component of the actomyosin interface in the strongly bound complex. Located within this helix are several partially exposed hydrophobic residues (I341, I345, L346) which have been proposed to play an important role in the rigor or strong interaction with myosin. In this study, we tested the structural and functional importance of individual residues in this helix in the interactions with myosin. Strikingly, the interaction with myosin was strongly affected by alanine substitution at I341 but not I345 on actin. The deficiency in the I341A actin was probably not due to any global structural changes in actin as the circular dichroism, intrinsic fluorescence, the polymerization by $MgCl_2$, and the weak binding of S1 to the I341A mutant were similar to those of wild-type actin. However, the 338−348 helix was sensitive to mutations as single or double substitution of either one or both residues to lysine or phenylalanine gave actins that were either dominantly or recessively lethal to the cell.

The strong binding of I341A mutant actin to S1 was reduced 9-fold compared to that of wild-type actin. In contrast to that, the I345A mutant actin showed no significant decrease in S1 binding. This shows that the proximal hydrophobic residues in the 338−348 helix have different contributions to the binding energy of the rigor actomyosin complexes. A recent report illustrates that the binding energy of a protein−protein complex can be derived from a small subset of residues located at the binding interface (Clackson & Wells, 1995). This study compared the loss of binding energy after mutation of individual residues located at the crystallographically determined interface of the human growth hormone and its receptor domain. Of 33 different residues substituted with alanine, only a small subset of amino acids, dominated by 2 tryptophans, was responsible for three-fourths of the binding energy of the complex.

Despite the decrease in the strong binding of the I341A actin to S1, there was no significant change in the weak binding of mutant actin to myosin in either cosedimentation, ATPase activities (K_m), or the *in vitro* motility assays. This result confirms the expectation that the binding energy for formation of the actomyosin interface under weak binding conditions is not derived from the same residues that dominate the strong acto−S1 binding (Rayment *et al.*, 1993).

Clearly, a change in the strong binding of S1 to actin may have a direct impact on the transition between the weakly

and strongly bound actomyosin states. Such a transition is believed to be central to the generation of force and the actomyosin ATPase cycle. Indeed, the V_{max} for I341A activation of myosin ATPase was reduced 4-fold while the K_m was unchanged compared to that of wild-type actin. This indicates that the reduction of equilibrium rigor binding can be coupled to the inhibition of the steady-state actomyosin ATPase. The step most likely affected by the mutation is the transition of the weakly bound actin·myosin·ADP·P_i to the strongly bound actin·myosin·ADP.

The sliding velocity of the I341A mutant actin filaments and the percentage of mobile filaments in the motility assay were smaller than those for wild-type actin filaments. The motion of the mutant actin filaments resembled the sliding of wild-type actin over a surface containing a mixture of HMM and load-bearing NEM-HMM. The first evidence that the reduced sliding of the mutant actins was due to some threshold mechanical load was provided by the restoration and improvement of its movement by ADP. It appears that the ADP-induced increase in the force-generating state (Pate *et al.*, 1993) allows the filament to overcome the threshold load and move smoothly over the surface. However, this indicates also that a mechanical load is present in the assay under standard assay conditions, despite the presence of the reducing agent (DTT) and carrier protein (BSA) to inhibit the photodamage of HMM.

An NEM-HMM external load method (Haeberle, 1994) enabled the comparison of actin filaments in the motility assay and revealed that the I341A actin was deficient in its mechanical interactions with myosin. A smaller amount of load-bearing NEM-HMM was necessary to halt the movement of the I341A actin filaments than that of wild-type actin. This suggested that about 40% less force was generated along the mutant actin filaments. However, the accuracy of such an estimate in the motility assay may be in question because internal load due to photodamage to HMM is not accounted for. In principal, the reduced force could be due to a smaller force generated per crossbridge or a decreased number of force-generating crossbridges in the mutant actomyosin ATPase cycle. The latter possibility is favored; it is consistent with the decreased transition of I341A actin from the weakly to strongly bound actomyosin complexes. However, future experiments, such as those using the optical laser trap (Finer *et al.*, 1994), can address more directly the question of force generation by testing the actomyosin interaction at the level of the single myosin crossbridge.

Previously, we and others investigated the impact of mutations in the weakly binding myosin sites of actin on the actomyosin cycle (Miller & Reisler, 1995; Sutoh *et al.*, 1991). The loss of charges in actin mutants D24A/D25A and E99A/E100A decreased the weak but not the strong binding of S1 to actin yet still allowed filaments to slide at velocities similar to those of wild-type actin. However, this sliding was dependent on the presence of methylcellulose in the motility assay buffer (Miller & Reisler, 1995). The methylcellulose was not required for the sliding of the I341A mutant filaments despite a 9-fold decrease in the strong binding. This suggests that the unimpaired weak binding of myosin to I341A actin enables filaments to remain attached to the HMM-coated surface during all steps of the actomyosin cycle. On the other hand, the decrease in the strong binding of myosin to I341A actin had a direct effect on the filament motion and the force generated in the *in vitro* motility assays. Thus, the I341A mutant is clearly distinct from the weak binding mutants in its myosin binding properties and, consequently, in its mechanical behavior. These results suggest that further mutagenic screening of actomyosin interface residues should lead to a detailed description of actomyosin cycle in terms of site- and residue-specific protein−protein interactions.

REFERENCES

Adams, S., & Reisler, E. (1993) *Biochemistry 32*, 5051−5056.

Aspenstrom, P., Engkvist, H., Lindberg, U., & Karlsson, R. (1992) *Eur. J. Biochem. 207*, 315−320.

Clackson, T., & Wells, J. A. (1995) *Science 267*, 383−386.

Cook, R. K., Root, D., Miller, C., Reisler, E., & Rubenstein, P. A. (1993) *J. Biol. Chem. 268*, 2410−2415.

Cooke, R. (1995) *FASEB J. 9*, 636−642.

Cooke, R., & Pate, E. (1985) *Biophys. J. 48*, 789−798.

Cuda, G., Fananapazir, L., Zhu, W. S., Sellers, J. R., & Epstein, N. D. (1993) *J. Clin. Invest. 91*, 2861−2865.

DasGupta, G., & Reisler, E. (1992) *Biochemistry 31*, 1836−1841.

Finer, J. T., Simmons, R. M., & Spudich, J. A. (1994) *Nature 368*, 113−119.

Godfrey, J. E., & Harrington, W. F. (1970) *Biochemistry 9*, 886−895.

Haeberle, J. R. (1994) *J. Biol. Chem. 269*, 12424−12431.

Haeberle, J. (1995) *Biophys. J. 4*,306S−310S.

Homsher, E., Wang, F., & Sellers, J. R. (1992) *Am. J. Physiol. 262*, C714−C723.

Ito, H., Fukuda, Y., Murata, K., & Kimura, A. (1983) *J. Bacteriol. 153*, 163−168.

Kabsch, W., Mannherz, H. G., Suck, D., Pai, E., & Holmes, K. C. (1990) *Nature 347*, 37−44.

Kaiser, C., Michaelis, S., & Mitchell, A. (1994) *Methods in Yeast Genetics*, CSHL Press, Cold Spring Harbor, NY.

Kodama, T., Fukui, K., & Kometani, K. (1986) *J. Biochem. 99*, 1465−1472.

Kron, S. J., Toyoshima, Y. Y., Uyeda, T. Q., & Spudich, J. A. (1991) *Methods Enzymol. 196*, 399−416.

Kunkel, T. A., Roberts, J. D., & Zakour, R. A. (1987) *Methods Enzymol. 154*, 367−382.

Labbe, J. P., Lelievre, S., Boyer, M., & Benyamin, Y. (1994) *Biochem. J. 299*, 875−879.

Laemmlli, U. K. (1970) *Nature 227*, 680−685.

Miller, C. J., & Reisler, E. (1995) *Biochemistry 34*, 2694−2700.

Pate, E., & Cooke, R. (1989) *J. Muscle Res. Cell Motil. 10*, 181−196.

Rayment, I., Holden, H. M., Whittaker, M., Yohn, C. B., Lorenz, M., Holmes, K. C., & Milligan, R. A. (1993a) *Science 261*, 58−65.

Rayment, I., Rypniewski, W. R., Schmidt-Base, K., Smith, R., Tomchick, D. R., Benning, M. M., Winkelmann, D. A., Wesenberg, G., & Holden, H. M. (1993b) *Science 261*, 50−58.

Sambrook, J., Fritsch, E. F., & Maniatis, T. (1989) *Molecular Cloning: A Laboratory Manual*, 2nd ed., Cold Spring Harbor Laboratory Press, Cold Spring Harbor, NY.

Sanger, F., Nicklen, S., & Coulson, A. R. (1977) *Proc. Natl. Acad. Sci. U.S.A. 74*, 5463−5467.

Schroder, R. R., Manstein, D. J., Jahn, W., Holden, H., Rayment, I., Holmes, K. C., & Spudich, J. A. (1993) *Nature 364*, 171−174.

Sikorski, R. S., & Hieter, P. (1989) *Genetics 122*, 19−27.

Spudich, J. A., & Watt, W. (1971) *J. Biol. Chem. 246*, 4866−4871.

Sutoh, K., Ando, M., & Toyoshima, Y. Y. (1991) *Proc. Natl. Acad. Sci. U.S.A. 88*, 7711−7714.

Vieira, J., & Messing, J. (1991) *Gene 100*, 189−194.

Warrick, H. M., Simmons, R. M., Finer, J. T., Uyeda, T. Q., Chu, S., & Spudich, J. A. (1993) *Methods Cell Biol. 39*, 1−21.

Warshaw, D. M., DeRosier, J. M., Work, S. S., & Trybus, K. M. (1991) *J. Biol. Chem. 266*, 24339−24343.

Weeds, A., & Pope, A. B. (1977) *J. Mol. Biol. 111*, 129−157.

Wertman, K. F., Drubin, D. G., & Botstein, D. (1992) *Genetics 132*, 337−350.

BI952645V